A Practical Palmprint Recognition Algorithm Using Phase Information

Satoshi Iitsuka, Koichi Ito and Takafumi Aoki
Graduate School of Information Sciences,
Tohoku University
Sendai-shi 980-8579, Japan
E-mail: {iitsuka, ito}@aoki.ecei.tohoku.ac.jp

Abstract

This paper proposes a practical palmprint recognition algorithm using two-dimensional (2D) phase information. The proposed algorithm (i) reduces the registered data size by registering quantized phase information and (ii) deals with nonlinear distortion between palmprint images by local block matching. Experimental evaluation using palmprint image databases clearly demonstrates efficient recognition performance of the proposed algorithm compared with the conventional palmprint recognition algorithms.

1 Introduction

A palmprint, the large inner surface of a hand, contains many features such as principle lines, ridges, minutiae points, singular points and texture, and is expected to be more distinctive than a fingerprint [9]. Conventional algorithms for palmprint recognition are to extract feature vectors corresponding to individual palmprint images and to perform palmprint matching based on some distance metrics [9, 1, 10]. We have proposed a palmprint recognition algorithm using Phase-Only Correlation (POC) which is an image matching technique using the phase components in 2D Discrete Fourier Transforms (DFTs) of given images [2]. The recognition performance of these algorithms is degraded for palmprint images having nonlinear distortion due to movement of a hand and fingers, since these algorithms consider only the rigid body transformation between palmprint images.

In this paper, we propose a practical palmprint recognition algorithm using 2D phase information. The proposed algorithm (i) reduces the registered data size by registering quantized phase information and (ii) deals with nonlinear distortion between palmprint images by local block matching using Phase-Only Correlation. Experimental evaluation using the PolyU Palmprint Database [5] demonstrates efficient recognition performance of the proposed algorithm compared with conventional algorithms.

2 Phase-Only Correlation

We introduce the principle of a Phase-Only Correlation (POC) function (which is sometimes called the "phase-correlation function") [4, 7, 8].

Consider two $N_1 \times N_2$ images, $f(n_1, n_2)$ and $g(n_1, n_2)$, where we assume that the index ranges are $n_1 = -M_1, \cdots, M_1$ ($M_1 > 0$) and $n_2 = -M_2, \cdots, M_2$ ($M_2 > 0$) for mathematical simplicity, and hence $N_1 = 2M_1 + 1$ and $N_2 = 2M_2 + 1$. The discussion could be easily generalized to non-negative index ranges with power-of-two image size. Let $F(k_1, k_2)$ and $G(k_1, k_2)$ denote the 2D DFTs of the two images. $F(k_1, k_2)$ is given by

$$\begin{aligned} F(k_1, k_2) &= \sum_{n_1, n_2} f(n_1, n_2) W_{N_1}^{k_1 n_1} W_{N_2}^{k_2 n_2} \\ &= A_F(k_1, k_2) e^{j\theta_F(k_1, k_2)}, \end{aligned} \quad (1)$$

where $k_1 = -M_1, \cdots, M_1$, $k_2 = -M_2, \cdots, M_2$, $W_{N_1} = e^{-j\frac{2\pi}{N_1}}$, $W_{N_2} = e^{-j\frac{2\pi}{N_2}}$, and $\sum_{n_1, n_2}$ denotes $\sum_{n_1=-M_1}^{M_1} \sum_{n_2=-M_2}^{M_2}$. $A_F(k_1, k_2)$ is amplitude and $\theta_F(k_1, k_2)$ is phase. $G(k_1, k_2)$ is defined in the same way. The cross-phase spectrum $R_{FG}(k_1, k_2)$ is given by

$$R_{FG}(k_1, k_2) = \frac{F(k_1, k_2)\overline{G(k_1, k_2)}}{|F(k_1, k_2)\overline{G(k_1, k_2)}|} = e^{j\theta(k_1, k_2)}, \quad (2)$$

where $\overline{G(k_1, k_2)}$ is the complex conjugate of $G(k_1, k_2)$ and $\theta(k_1, k_2)$ denotes the phase difference $\theta_F(k_1, k_2) - \theta_G(k_1, k_2)$. The POC function $r_{fg}(n_1, n_2)$ is the 2D Inverse DFT (2D IDFT) of $R_{FG}(k_1, k_2)$ and is given

978-1-4244-2175-6/08/$25.00 ©2008 IEEE

by

$$r_{fg}(n_1,n_2) = \frac{1}{N_1 N_2} \sum_{k_1,k_2} R_{FG}(k_1,k_2) W_{N_1}^{-k_1 n_1} W_{N_2}^{-k_2 n_2}, \quad (3)$$

where $\sum_{k_1,k_2}$ denotes $\sum_{k_1=-M_1}^{M_1} \sum_{k_2=-M_2}^{M_2}$. When two images are similar, their POC function gives a distinct sharp peak. When two images are not similar, the peak drops significantly. The height of the peak gives a good similarity measure for image matching, and the location of the peak shows the translational displacement between the images.

We have proposed a BLPOC (Band-Limited Phase-Only Correlation) function [3] dedicated to biometric authentication tasks. The idea to improve the matching performance is to eliminate meaningless high frequency components in the calculation of cross-phase spectrum R_{FG} depending on the inherent frequency components of palmprint images. Assume that the ranges of the inherent frequency band are given by $k_1 = -K_1, \cdots, K_1$ and $k_2 = -K_2, \cdots, K_2$, where $0 \leq K_1 \leq M_1$ and $0 \leq K_2 \leq M_2$. Thus, the effective size of frequency spectrum is given by $L_1 = 2K_1 + 1$ and $L_2 = 2K_2 + 1$. The BLPOC function is given by

$$\begin{aligned} r_{fg}^{K_1 K_2}(n_1,n_2) &= \frac{1}{L_1 L_2} {\sum_{k_1,k_2}}' R_{FG}(k_1,k_2) \\ &\quad W_{L_1}^{-k_1 n_1} W_{L_2}^{-k_2 n_2}, \end{aligned} \quad (4)$$

where $n_1 = -K_1, \cdots, K_1$, $n_2 = -K_2, \cdots, K_2$, and $\sum'_{k_1,k_2}$ denotes $\sum_{k_1=-K_1}^{K_1} \sum_{k_2=-K_2}^{K_2}$. Note that the maximum value of the correlation peak of the BLPOC function is always normalized to 1 and does not depend on L_1 and L_2. In this paper, we employ $K_1/M_1 = K_2/M_2 = 0.5$.

3 Enrollment Stage

The proposed palmprint recognition algorithm consists of the enrollment and matching stages. This section describes the enrollment stage which consists of (i) preprocessing and (ii) feature extraction.

(i) Preprocessing

This step is to extract the palmprint region from an input image. In order to extract the center part of a palmprint for accurate matching, we employ the method described in Ref. [10]. This method uses gaps between fingers as reference points to define the palmprint region as shown in Fig. 1 (a). Figure 1 (b) shows the extracted palmprint region $f(n_1,n_2)$, where the size of palmprint region is 128×128 pixels in this paper.

(ii) Feature extraction

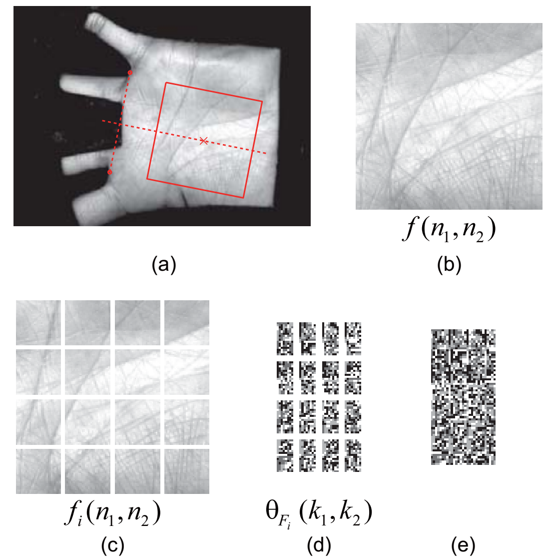

Figure 1. Enrollment stage: (a) input image and extracted palmprint region, (b) extracted palmprint region, (c) local block images, (d) phase information of each local block image and (e) registered data.

In local blocks of palmprint regions, the nonlinear distortion is approximately represented by the translational displacement between local blocks. According to this fact, the palmprint features registered in the database is generated as follows: (i) partition the palmprint region $f(n_1,n_2)$ into local blocks (Fig. 1 (c)), where the block size is 32×32 pixels and the number of local blocks is 16 in this paper, (ii) compute the phase spectrum of local blocks by 2D DFT (Fig. 1 (d)) and (iii) eliminate the meaningless high frequency components and reduce the size of phase information based on the symmetry property of DFT and quantization. The upper half of the phase components is eliminated, since the parameter of the BLPOC function is $K_1/M_1 = K_2/M_2 = 0.5$. The size of local phase features is 130 pixels in this paper. The palmprint features registered in the database is the combined phase features as shown in Fig. 1 (e).

4 Matching Stage

The matching stage consists of two steps: (i) preprocessing and (ii) matching. The preprocessing of the matching stage is almost the same process as that of the enrollment stage. The matching is performed by local block matching using POC.

(i) Preprocessing

In order to align the local blocks, the palmprint region $g(n_1,n_2)$ extracted from the input image is larger

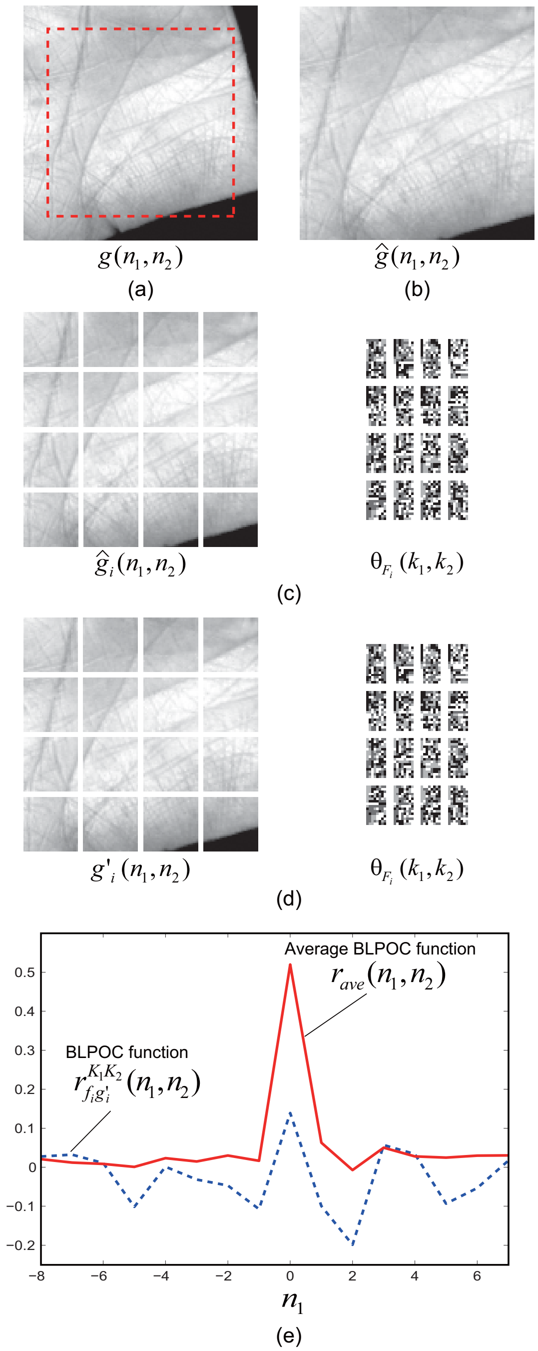

Figure 2. Matching stage: (a) input image, (b) extracted palmprint region, (c) image blocks $\hat{g}_i(n_1, n_2)$ and registered data, (d) aligned image blocks $g'_i(n_1, n_2)$ and registered data and (e) BLPOC function and average BLPOC function where $n_2 = 0$.

than that of the registered palmprint region $f(n_1, n_2)$. In this paper, the size of $g(n_1, n_2)$ is 160×160 pixels as shown in Fig. 2 (a). Note that the 128×128-pixel palmprint region $\hat{g}(n_1, n_2)$ extracted from $g(n_1, n_2)$ is used in the next step.

(ii) Matching

This step is to evaluate the similarity between two palmprint regions taking account of nonlinear distortion as follows. The palmprint region $\hat{g}(n_1, n_2)$ is separated into 32×32-pixel blocks as shown in Fig. 2 (c). Each block is indicated by $\hat{g}_i(n_1, n_2)$ $(i = 1, \cdots, N_{block})$. The translational displacement (δ_1, δ_2) between $\hat{g}_i(n_1, n_2)$ and $\theta_{F_i}(k_1, k_2)$ is estimated using the BLPOC function. The 32×32-pixel blocks $g'_i(n_1, n_2)$ are extracted from the palmprint region $g(n_1, n_2)$ as

$$g'_i(n_1, n_2) = g(n_1 - \delta_1, n_2 - \delta_2). \qquad (5)$$

The BLPOC functions $r^{K_1K_2}_{f_ig'_i}(n_1, n_2)$ between $g'_i(n_1, n_2)$ and $\theta_{F_i}(k_1, k_2)$ are computed. In order to improve the recognition accuracy of the BLPOC functions, we take the average of a set of the BLPOC functions as follows

$$r_{ave}(n_1, n_2) = \sum_{i=1}^{N_{block}} r^{K_1K_2}_{f_ig'_i}(n_1, n_2)/N_{block}. \qquad (6)$$

Figure 2 (e) shows an example of PNR (Peak-to-Noise Ratio) improvement through averaging [6]. The matching score between $f(n_1, n_2)$ and $g(n_1, n_2)$ is obtained as the highest peak value of $r_{ave}(n_1, n_2)$.

5 Experiments and Discussion

This section describes a set of experiments using 1st version and 2nd version of the PolyU palmprint database [5] for evaluating palmprint recognition performance of the proposed algorithm. The 1st version consists of 600 images (384×284 pixels) with 100 subjects and 6 different images of each palmprint. On the other hand, the 2nd version consists of 7,752 images (384×284 pixels) with 386 subjects and about 20 different images of each palmprint.

The performance of the biometrics-based verification system is evaluated by the Receiver Operating Characteristic (ROC) curve, which illustrates the False Non-Match Rate (FNMR) against the False Match Rate (FMR) at different thresholds on the matching score. We first evaluate the FNMR for all the possible combinations of genuine attempts; the number of attempts is ${}_6C_2 \times 100 = 1,500$ for 1st version and 74,068 for 2nd version. Next, we evaluate the FMR for all the possible combinations of impostor attempts; the number of attempts is ${}_{600}C_2 - 1,500 = 178,200$ for 1st version

Table 1. Experimental results of algorithms (A) and (B) for 1st version.

	EER [%]	Data size [byte]	Time [sec.]
(A)	2.147	4,096	0.40
(B)	0.200	5,929	0.29

Table 2. Experimental results of algorithm (C) for 1st version.

Quantization level [bit]	EER [%]	Data size [byte]
2	0.132	520
3	0.003	780
4	0.012	1,040
5	0.009	1,300
6	0.010	1,560
7	0.009	1,820
8	0.010	2,080
Time [sec.]	0.30	

and ${}_{7,752}C_2 - 74,068 = 29,968,808$ for 2nd version. The performance is also evaluated by the Equal Error Rate (EER), which is defined as the error rate where the FNMR and the FMR are equal. The computation time of the algorithm is evaluated by using MATLAB 7.2.0 on Intel Core2 Duo E6850 (3.00GHz$\times$2).

For the 1st version of the PolyU Palmprint database, we compare three different matching algorithms: (A) Zhang's algorithm [10], (B) our conventional algorithm [2] and (C) the proposed algorithm. The experimental results are shown in Tables 1 and 2. The proposed algorithm (C) exhibits significantly efficient performance, since the EER is low, the registered data size is small and the computation time is fast compared with the conventional algorithms (A) and (B).

For the 2nd version of the PolyU Palmprint database, we compare the proposed algorithm (C) with the conventional algorithm (A) in Ref. [10]. In this experiment, we evaluate the performance of the proposed algorithm using the same data set of Ref. [10]. Table 3 shows the experimental results. The reported value of EER in Ref. [10] is 0.6%, while the EERs of the proposed algorithm are below 0.37%. As is observed in the above experiments, the proposed algorithm is particularly useful for recognizing palmprint images.

6 Conclusion

This paper has proposed the practical palmprint recognition algorithm using phase information. Experimental results demonstrate efficient recognition performance of the proposed algorithm compared with the conventional algorithms.

Table 3. Experimental results of algorithm (C) for 2nd version.

Quantization level [bit]	EER [%]
2	0.364
3	0.252
4	0.227
5	0.234
6	0.235
7	0.227
8	0.224

References

[1] N. Duta, A. Jain, and K. Mardia. Matching of palmprints. *Pattern Recognition Letters*, 23(4):477–485, 2002.

[2] K. Ito, T. Aoki, H. Nakajima, K. Kobayashi, and T. Higuchi. A palmprint recognition algorithm using phase-only correlation. *IEICE Trans. Fundamentals*, E91-A(4):1023–1030, Apr. 2008.

[3] K. Ito, H. Nakajima, K. Kobayashi, T. Aoki, and T. Higuchi. A fingerprint matching algorithm using phase-only correlation. *IEICE Trans. Fundamentals*, E87-A(3):682–691, Mar. 2004.

[4] C. D. Kuglin and D. C. Hines. The phase correlation image alignment method. *Proc. Int. Conf. Cybernetics and Society*, pages 163–165, 1975.

[5] PolyU Palmprint Database, http://www4.comp.polyu.edu.hk/˜biometrics/.

[6] T. Shibahara, T. Aoki, H. Nakajima, and K. Kobayashi. A sub-pixel stereo correspondence technique based on 1D phase-only correlation. *Proc. the 2007 IEEE Int. Conf. Image Processing*, pages V–221–V–224, Sept. 2007.

[7] K. Takita, T. Aoki, Y. Sasaki, T. Higuchi, and K. Kobayashi. High-accuracy subpixel image registration based on phase-only correlation. *IEICE Trans. Fundamentals*, E86-A(8):1925–1934, Aug. 2003.

[8] K. Takita, M. A. Muquit, T. Aoki, and T. Higuchi. A sub-pixel correspondence search technique for computer vision applications. *IEICE Trans. Fundamentals*, E87-A(8):1913–1923, Aug. 2004.

[9] D. Zhang. *Palmprint Authentication*. Kluwer Academic Publication, 2004.

[10] D. Zhang, W.-K. Kong, J. You, and M. Wong. Online palmprint identification. *IEEE Trans. Pattern Anal. Machine Intell.*, 25(9):1041–1050, Sept. 2003.